International Journal Of Engineering Research And Development
e- ISSN: 2278-067X, p-ISSN: 2278-800X, www.ijerd.com
Volume 20, Issue 2 (February. 2024), PP. 65-72

Local Structure and Optical Studies of Mn^{2+} Doped $[NH_4][Zn(HCOO)_3]$ Hybrid Formate Single Crystal

Maroj Bharati [a], Vikram Singh [a], Ram Kripal [b]
[a] *Department of Physics, Nehru Gram Bharti (DU), Jamunipur, Prayagraj, India*
[b] *EPR Laboratory, Department of Physics, University of Allahabad, Prayagraj-211002, India*
Tel: 91-532-2470532; Fax: 91-532-2460993
E-mail: marojbharati99@gmail.com, vikram.singh@ngbu.edu.in, ram_kripal2001@rediffmail.com

Abstract
Based on perturbation theory and the superposition model, the splitting parameters for the zero field of Mn^{2+} incorporated [NH4][Zn(HCOO)3] crystals are found. The acquired parameters fairly correspond to the experimental ones when the computation takes local distortion into account. The theoretical result supports the experimental finding that Mn^{2+} ion enters the $[NH_4][Zn(HCOO)_3]$ hybrid formate at substitutional Zn^{2+} site. The system's optical spectra are computed using the crystal field parameters from the superposition model and the crystal field analysis program. Through diagonalization of the entire Hamiltonian in the coupling scheme of intermediate crystal field, the energy band locations of the Mn^{2+} ion are derived. The Coulomb interaction, crystal field Hamiltonian, Trees correction, spin-orbit, spin-spin, and spin-other- orbit interactions make up the Hamiltonian,.the parameters B and C are employed in relation to the coulomb interaction. The calculated and experimental band positions are found to reasonably agree. As a result, the theoretical analysis validates the results of the experiment..

Keywords: *Organic compounds, Single crystal, Crystal fields, Electron paramagnetic resonance, Zero field splitting.*

Date of Submission: 12-02-2024 Date of Acceptance: 26-02-2024

I. Introduction

When a magnetic field is applied externally, one can use the method of electron paramagnetic resonance (EPR) to ascertain the transition metal ions' energies as they go through Zeeman transitions. Mn^{2+} ion is the most studied transition metal ions because of providing the EPR signal even in ambient conditions. This ion has half filled 3d orbital and its ground state is $^6S_{5/2}$. This ion's paramagentism can only be attributed to the electron spin because the angular momentum is zero. The zero field splitting of this ion in crystals shows sensitiveness to small structural changes of the system [1-3].

For use in EPR [4-6] and optical spectroscopy [7-8], the parameters for zero field splitting (ZFS) and crystal field (CF) can be semi-empirically modeled utilizing the superposition model (SPM). In [9], the spin Hamiltonian (SH) together with other Hamiltonians is explained. The parameters of the crystal field (CF) are often found employing SPM and the point-charge model [10] even if the exchange charge model (ECM) is a useful technique as well for analysing the effects of crystal fields in single crystals infused with rare earth and transition ions [11].. In this study, we used SPM to compute the ZFS parameters and B_{kq}, the CF parameters. SPM was suggested [12] for CF based on the ensuing presumptions: (1) An algebraic total of the crystal's other ions' contributions can be used to determine the paramagnetic ion's CF. All the significant contributions to the conservation of free energy from each paramagnetic ion have axial symmetry with respect to their position vector when the ion is in the chosen coordinate system's origin. (3) The CF contributions of just nearby or coordinated ions are to be taken into account. (4) Across various host crystals, contributions to CF from a solitary ion (ligand) can be transmitted. The axial symmetry assumption, however (2) permits the transformation of one coordinate system into another, the first assumption provides support for the applicability of superposition principle in characterising the CF. Nonetheless, a more limited version of assumption (3) is sometimes utilised, when solely the closest neighbour ions are occupied. According to the final ligand transferability assumption (4), the only factors influencing the contributions of one ion to CF are its character and separation from the paramagnetic ion. In order to perform an SPM analysis on the CF, it is essential to obtain a stable polar coordinate system (R_L, θ_L, Φ_L) for each ligand or ion from the host crystal's X-ray data. When transition metal ions are doped, ionic size, ionic charge, and inter-ionic bonding mismatches will probably result in some degree of local distortion. To find the fitted values of the SPM power-law exponents and

the intrinsic parameters, a non-linear or linear least-square fit may be performed on an adequate quantity of CF parameters. Mn^{2+} and Fe^{3+} experimental spin-Hamiltonian parameters in CaO and MgO crystals have been critically analysed [13]. For the EPR data, it gives the SPM parameters' exact values. and demonstrates that the superposition principle is satisfied by the CF for 3d ions. A strict lattice relaxation model was utilised [14] to ascertain sets of SPM intrinsic parameters based on dependable ligand distances for the oxides of alkali earth. For Fe^{3+} and Mn^{2+} doped MgO, CaO, and SrO (R0 = 2.0 Å): $\overline{b_2}$ = (-1552±48) $\times 10^{-4}$ cm^{-1} and (-6440±113) $\times 10^{-4}$ cm^{-1}, respectively, with a fixed t_2 = 16 for both ions. For both Fe^{3+} and Mn^{2+}, the values of $\overline{b_4}$ are 9.9±0.8 $\times 10^{-4}$ cm^{-1}, with a fixed t_4 of 16±4 for each ion. The fitted values for Mn^{2+} and Fe^{3+}, respectively, were 17.7 and 14.4 for the separate fitting of t_2.

Because of their hybrid inorganic-organic nature, the recently created metal-organic frameworks (MOFs) have demonstrated a variety of properties or functionalities [15]. MOFs are widely researched hybrid materials because of their possible applications in drug delivery systems, multiferroic memory devices, and separation and gas storage devices [16–19]. These networks of coordination are made up of metal centers that form porous structures and various organic linker molecules. The pore system in the dense MOFs confines molecules firmly attached to the structure [15]. The [A][M(HCOO)3] metal-formates, which show intriguing ferromagnetic and ferroelectric-like properties, are the most significant class of dense MOFs [18–21]. The aforementioned compounds' metal centers M^{2+} (Zn^{2+}, Cd^{2+}, and Mg^{2+} ions) are joined into anionic frameworks with MO_6 octahedra by formate linkers [22–25]. Molecular cations A^+ such as $(CH_3)_2NH_2^+$ [18–19, 20, 22] or NH_4^+ [23, 24] are contained by these porous structures. Structural order-disorder phase transitions are a common property shared by most formate frameworks [20, 22-25]. A ferroelectric behavior was found in $[NH_4][M(HCOO)_3]$ frameworks having ammonium (NH_4^+) cations [23, 26, 27]. These systemss generally crystallize in 4^9 - 6^6 chiral structural topology, which is less common [28] with the possible 4^{12}–6^3 topology [NH4][Cd(HCOO)3] framework being an exception [29]. $[NH_4][Zn(HCOO)_3]$ (AmZn) is an interesting example of above frameworks. The ammonium cation ordering and change of space group from $P6_322$ in the high temperature (HT) phase ($T > T_0$) to the polar $P6_3$ in the low temperature (LT) phase ($T < T_0$) occur after this experiences a structural phase change at roughly T_0 = 190 K [27].

One AmZn crystal doped with Mn^{2+} has undergone EPR analysis from 26-332 K [30], and ZFS parameters D and E have been established at 100 and 26 K. The results suggest that the substitutional Zn^{2+} site in AmZn is occupied by Mn^{2+} ions [33]. In the current study, the ZFS parameters D and E are calculated for the Mn^{2+} ion in AmZn at substitutional Zn^{2+} site at 100 K using CF parameters evaluated from SPM and perturbation equations [31]. The objective is to find the location of Mn^{2+} ion and the distortion occurring in the crystal. The results found for the Mn^{2+} ion at substitutional Zn^{2+} site in AmZn crystal with local distortion provide reasonable match with the experimental values. Additional objective of the present study seeks to determine the extent to which CF theory and SPM analysis can be applied to Mn^{2+} ions in AmZn crystals in order to create an SPM parameter database. Molecular nanomagnet (MNM) design and computer modeling of their magnetic and spectroscopic characteristics will be determined by this. SMMs, or single-molecule magnets, [32], single-chain magnets (SCM) [33], and single ion magnets (SIM) [34] are currently included in the transition ion-based MNM class. The above systems have drawn large attention because of the noteworthy magnetic characteristics of MNM, for instance, magnetization's macroscopic quantum tunneling and potential uses in quantum computing and high-density information storage [32, 33]. There have been numerous synthesized SCM or SMM systems with $Mn^{2+}$and Cr^{3+} ions [35]. The parameters of the model established in this case may be used for ZFS parameter calculations for Mn^{2+} ions at similar sites in MNM, since model calculations for simpler crystal systems can serve as a foundation for more complex ones. The modeling employed in this work can be extended to explore crystals of scientific and industrial interest in numerous other ion-host systems.

II. Crystal Structure

AmZn's structures at 290 and 110 K have been identified [27]. The crystal has a nonpolar point group D6, a hexagonal space group $P6_322$ at 290 K, with a = 7.3084(2) Å, c = 8.1705(3) Å, and V = 377.94(2) $Å^3$. The structure $[NH_4][M(HCOO)_3]$ (M = Mn^{2+}, Co^{2+}, Ni^{2+}) [28] is identical,. It has a (4^9 - 6^6) network topology and a three-dimensional array of NH_4^+ cations in a chiral anionic [Zn(HCOO)3-] framework placed along the c direction in its helical channels [36]. At 190 K, a structural phase change that occurs in AmZn was observed, which was succeeded by the disorder-order transition of NH_4^+ and associated structural changes, as well as the unit cell tripling with the polar $P6_3$ replacing $P6_322$ as the space group. While a at 110 K becomes 12.5919(3) Å very close to $3^{1/2}$ a at 290 K, compared to 290 K, the length of c is marginally longer at 110 K (8.2015(2) Å). As a result, V at 110 K = 1126.18(5) $Å^3$, which is almost equal to 3V at 290 K. The AmZn crystal structure at 110 K is displayed in Fig. 1 adopting an axis system with symmetry (SAAS).

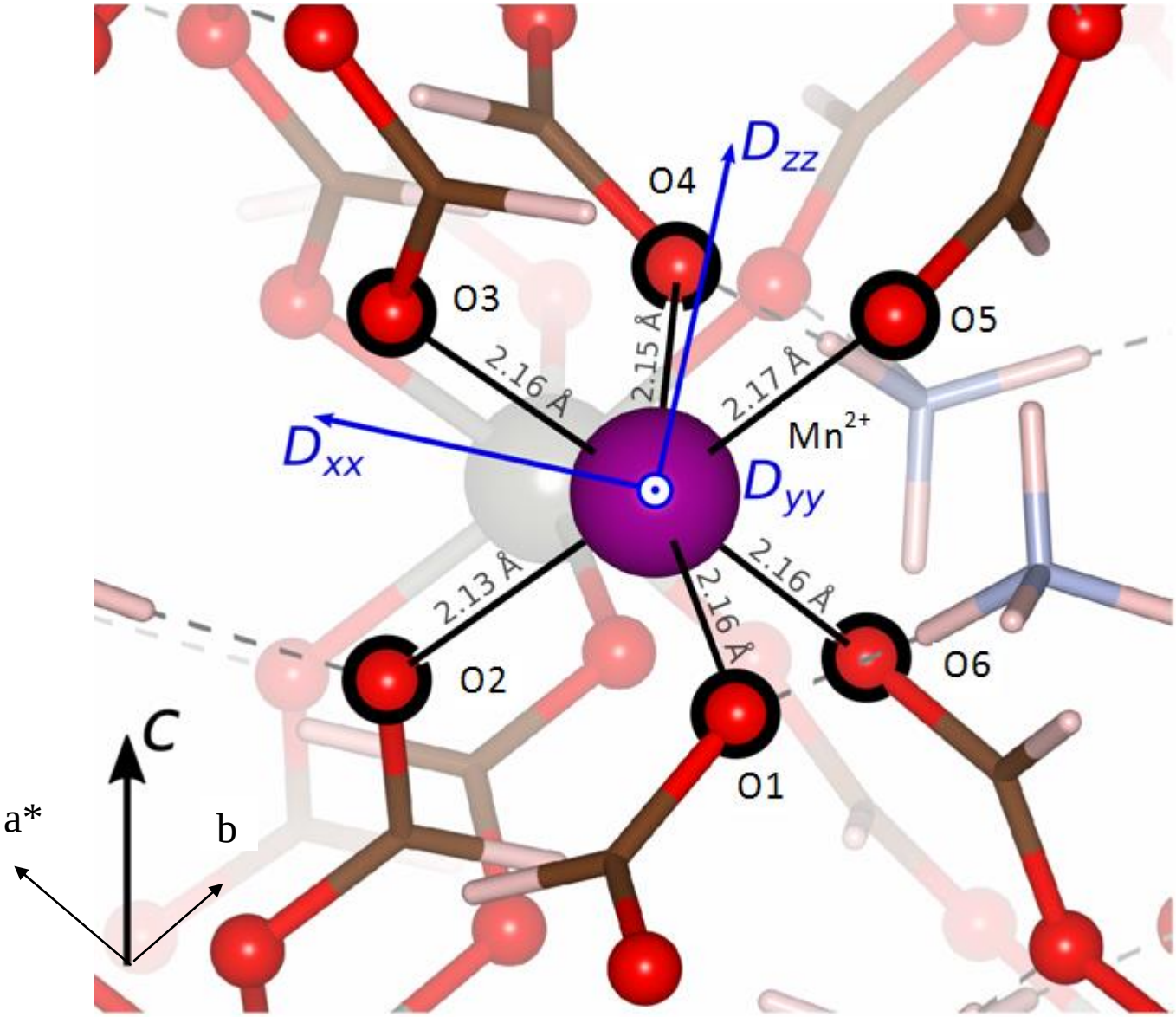

Fig. 1. AmZn crystal structure at 110 K adopting an axis system with symmetry (SAAS).

III. Crystal Field and Zero Field Splitting Parameter Calculations

The analysis of EPR spectra is done with the spin Hamiltonian [5] given below:

$$\mathcal{H} = \mu_B B.g.S + D\left\{S_Z^2 - \frac{1}{3}S(S+1)\right\} + E(S_x^2 - S_y^2) \qquad (1)$$

where B, μ_B, g, D and E are the applied magnetic field, Bohr magneton, splitting factor, second rank axial, and second rank rhombic ZFS parameters [37–38]. The a*, b, and c modified crystal axes are along the laboratory axes (x, y, z). The directions of metal-ligand bonds that are mutually perpendicular are referred to as the local symmetry axes of the site or the symmetry adopted axes (SAA). As demonstrated in Fig.1, the axis-Z of SAAS is along the crystal axis- c, and (X, Y) are perpendicular to the axis-Z. When Mn^{2+} ions are doped in AmZn crystal, these enter the lattice at substitutional Zn^{2+} sites with some local distortion [39].

For a $3d^5$ ion, the spin Hamiltonian can be expressed as [40],

$$\mathcal{H} = \mathcal{H}_o + \mathcal{H}_{so} + \mathcal{H}_{ss} + \mathcal{H}_c \qquad (2)$$

$$\mathcal{H}_c = \sum B_{kq} C_q^{(k)} \qquad (3)$$

where B_{kq}, in Wybourne notation, are the CF parameters and $C_q^{(k)}$ are the spherical tensor operators of Wybourne. $B_{kq} \neq 0$ in the orthorhombic symmetry crystal field only for k = 2, 4; q = 0, 2, 4. Utilizing SPM, the CF parameters B_{kq} are computed [41].

The symmetry of the local field about Mn^{2+} ions in the AmZn crystal is assumed to be orthorhombic (OR-type I) [5]. In OR-type I symmetry, the ZFS parameters D and E are ascertained as follows [41

$$D = \left(\frac{3\varsigma^2}{70P^2D'}\right)[-B_{20}^2 - 21\varsigma B_{20} + 2B_{22}^2] + \left(\frac{\varsigma^2}{63P^2G}\right)[-5B_{40}^2 - 4B_{42}^2 + 14B_{44}^2] \quad (4)$$

$$E = \left(\frac{\sqrt{6}\varsigma^2}{70P^2D'}\right)[2B_{20} - 21\varsigma]B_{22} + \left(\frac{\varsigma^2}{63P^2G}\right)[3\sqrt{10}B_{40} + 2\sqrt{7}B_{44}]B_{42} \quad (5)$$

In above Eqns. P = 7B+7C, G = 10B+5C, D' = 17B+5C. B and C are Racah parameters and ς is the spin-orbit coupling parameter. With the average covalency parameter N in mind, we get $B = N^4B_0$, $C = N^4 C_0$, $\varsigma = N^2 \varsigma_0$, where ς_0 presents free ion spin-orbit coupling parameter and B_0 and C_0 Racah parameters for free ion [40, 42]. For free Mn^{2+} ion, $B_0 = 960$ cm^{-1}, $C_0 = 3325$ cm^{-1} and $\varsigma_0 = 336$ cm^{-1} [5].

The parameter N is evaluated from $N = (\sqrt{B/B_0} + \sqrt{C/C_0})/2$ taking Racah parameters (B = 906 cm^{-1}, C = 2254 cm^{-1}) found through optical analysis of Mn^{2+} ion in the crystal with oxygen ligands [43].

The CF parameters, in terms of co-ordination factor $K_{kq}(\theta_j, \varphi_j)$ and intrinsic parameter $\overline{A_k}(R_j)$, using SPM are found [12, 41] as

$$B_{kq} = \sum_j \overline{A_k}(R_j) K_{kq}(\theta_j, \phi_j) \quad (6)$$

$\overline{A_k}(R_j)$, the intrinsic parameter, is provided by

$$\overline{A_k}(R_j) = \overline{A_k}(R_0)\left(\frac{R_0}{R_j}\right)^{t_k} \quad (7)$$

where R_j is the ligand's distance from the d^n ion, $\overline{A_k}(R_0)$ is the intrinsic parameter, R_0 is the reference distance of the ligand from the metal ion and t_k denotes power law exponent. For Mn^{2+}doped crystals, $t_2 = 3$ and $t_4 = 7$ are used [41]. Different values are considered in the present calculation as discussed later. As the co-ordination about Mn^{2+} ion is octahedral for site I, $\overline{A_4}$ is found from the relation [44]

$$\overline{A_4}(R_0) = \frac{3}{4}Dq \quad (8)$$

Taking optical study [43], $Dq = 756$ cm^{-1}. Therefore, $\overline{A_4}(R_0) = 567$ cm^{-1}. For $3d^5$ ions the $\frac{\overline{A_2}}{\overline{A_4}}$ falls in the range 8 - 12 [40, 45-46]. Considering $\frac{\overline{A_2}}{\overline{A_4}} = 10$, $\overline{A_2} = 5670$ cm^{-1}.

IV. Results and Discussion

Using SPM, parameters $\overline{A_2}$ and $\overline{A_4}$, and the ligand arrangement around the Mn^{2+} ion as indicated in Fig. 1, the CF specifications of the Mn^{2+} ion at the substitutional Zn^{2+} site are computed. Table 1 provides atomic coordinates in AmZn single crystal along with bond length R (both with and without distortion) and angles θ, φ for site I. The CF parameters using Eq. (6) and ZFS parameters from Eqs. (4) & (5) along with reference distance R_0 are presented in Table 2. Table 2 demonstrates that $R_0 = 0.200$ nm is somewhat less than the sum of radii of ions (0.223 nm) of $Mn^{2+} = 0.083$ nm and $O^{2-} = 0.140$ nm along with no distortion yield ZFS parameters for substitutional octahedral site I to be larger than the experimental values [30]. |E|/|D| is also larger

than the standard value 0.33 [38]. Therefore, local distortion was taken into account. Using above value of R_0 and local distortion, the ZFS parameters for substitutional octahedral site I are in good accord with those from the experiment [30]. The parameters $t_2 = 18$ and $t_4 = 21$ with transformation S2 for standardization [38] have been used to obtain |E|/|D| ratio < 0.33 and calculated ZFS parameters near to experimental values.

Table 1. Atomic coordinates, bond length R (both with and without distortion), and angles θ, φ in AmZn single crystal (site I).

Position of Mn^{2+}	Ions	Spherical polar co-ordinates of ions								
		x	y	z	R(nm)		θ^0		φ^o	
		(Å)								
		Without distortion								
Substitutional	O1	0.42572	0.26472	0.44203	0.2088	R_1	93.96	θ_1	87.51	φ_1
Zn1	O2	0.42814	0.15518	0.23013	0.4174	R_2	94.89	θ_2	88.72	φ_2
(0.33522, 0.33146,	O3	0.39868	0.48889	0.44032	0.2101	R_3	93.98	θ_3	88.26	φ_3
0.58625)	O4	0.50569	0.60248	0.22882	0.4186	R_4	94.89	θ_4	87.65	φ_4
	O5	0 .17529	0.23515	0.44583	0.2100	R_5	93.83	θ_5	94.37	φ_5
	O6	0.06942	0.24422	0.23442	0.4130	R_6	94.88	θ_6	93.70	φ_6
		With distortion								
Site I	O1				0.3888		95.16		89.01	
	O2				0.4974		96.89		90.72	
	O3				0.3901		95.48		90.26	
	O4				0.4986		102.89		81.99	
	O5				0.3950		95.83		94.37	
	O6				0.4980		96.88		95.70	

Table 2. The Mn^{2+} doped AmZn crystal's zero field splitting and crystal field parameters.

		CF parameters (cm^{-1})						ZFS parameters ($\times 10^{-4} cm^{-1}$)		
Site	R_0(nm)	B_{20}	B_{22}	B_{40}	B_{42}	B_{44}	|D|	|E|	|E|/|D|	
		Without distortion								
Site I $\frac{A_2}{A_4}$ =10	0.200	-16399.9	-20176.8	3523.559	3729.196	6406.725	3540.3	1764.2	0.498	
		With distortion								
Site I $\frac{A_2}{A_4}$ =10	0.200	-0.10711	0.083849	0.003561	0.003815	1816.461	56.78	0.0009	1.706×10^{-4}	
						Exp.	56.78	9.35	0.164	

The CFA program [47] and B_{kq} parameters (with distortion) are used to compute the Mn^{2+} doped AmZn single crystals' optical spectra.. After diagonalizing the entire Hamiltonian, the locations of the energy bands of the Mn^{2+} ion are found. Table 3 displays the energy band positions for substitutional site I based on calculations and experimental data [43].

Table 3. The locations of Energy bands of single crystal of AmZn doped Mn^{2+}, both calculated and experimental.

From $^6A_{1g}(S)$ transition	Bands Observed (cm^{-1})	Bands Calculated (cm^{-1}) I
$^4T_{1g}(G)$	16044	20815, 20822, 21611, 21625, 21638, 21649
$^4T_{2g}(G)$	20433	21895, 21896, 21904, 21920, 21953, 21954
$^4E_g(G)$	24108	22618, 22621, 22624, 22630
$^4A_{1g}(G)$	24242	23428, 23430
$^4T_{2g}(D)$	26724	27208, 27222, 27256, 27268, 27294, 27303
$^4E_g(D)$	30451	30631, 30729, 30793, 30798
$^4T_{1g}(P)$	33956	32861, 32928, 32931, 33254, 33273, 33676
$^4A_{2g}(F)$	36846	36832, 36846
$^4T_{1g}(F)$	38521	37012, 37023, 37028, 37041, 37054, 39757

Table 3 shows that the calculated and experimental energy band positions agree fairly well. Therefore, the theoretical findings corroborate the experimental finding [30, 43] that Mn^{2+} ions enter the AmZn hybrid framework at substitutional octahedral sites. The model parameters available here may be used in ZFS parameter computations for Mn^{2+} ions at comparable MNM sites.

V. Conclusions

We have estimated zero field splitting parameters using perturbation theory and the superposition model for AmZn single crystals doped with Mn^{2+} ions. The ZFS parameters that were computed and the experimental values agree well. The estimated positions of the optical energy bands agree reasonably well with those from the experiment. Thus, experimental observation is supported by the theoretical results that Mn^{2+} ions occupy substitutional site I in AmZn hybrid framework. The model parameters obtained in this study may be used for ZFS parameter computations for Mn^{2+} ions at comparable locations in molecular nano magnets. The current modeling methodology can be extended to explore crystals for scientific and industrial purposes in numerous other ion-host systems.

Acknowledgement

The authors are grateful to the Head of Physics Department of Allahabad University, Allahabad for giving facilities of the department and to Prof. C. Rudowicz of Faculty of Chemistry, Adam Mickiewicz University, Poznan, Poland to send CFA program.

Declarations

Ethical Approval:

This research did not contain any studies involving animal or human participants, nor did it take place on any private or protected areas. No specific permissions were required for corresponding locations.

Competing interests:

The authors declare that they have no known competing financial interests or personal relationships that could have appeared to influence the work reported in this paper.

Authors' contributions:
Maroj Bharati and Vikram Singh- performed calculations, wrote the manuscript and prepared the figure.
Ram Kripal- idea and supervision.
All authors have reviewed the manuscript.

Funding:
No funding is received.
Availability of data and materials:
The data will be made available on request.

References

[1]. J. A. Weil, J. R. Bolton, Electron Paramagnetic Resonance: Elementary Theory and Practical Applications; 2nd ed., Wiley, New York, 2007.
[2]. F. E. Mabbs, D. Collison, D. Gatteschi, Electron Paramagnetic Resonance of d Transition Metal Compounds; Elsevier, Amsterdam, 1992.
[3]. R. M. Krishna, V. P. Seth, S. K. Gupta, D. Prakash, I. Chand, J. L. Rao, EPR of Mn^{2+}-ion-doped single crystals of $Mg[C_4H_3O_4]_2{\cdot}6H_2O$, Spectrochim. Acta A **53** (1997) 253-258.
[4]. C. Rudowicz, P. Gnutek, M. Açıkg¨oz, Superposition model in electron magnetic resonance spectroscopy – a primer for experimentalists with illustrative applications and literature database, Appl. Spectrosc. Rev. 54 (2019) 673–718.
[5]. A. Abragam, B. Bleaney, Electron Paramagnetic Resonance of Transition Ion, Dover, New York, 1986.
[6]. J.R. Pilbrow, Transition-Ion Electron Paramagnetic Resonance, Clarendon Press, Oxford, 1990.
[7]. B. G. Wybourne, Spectroscopic Properties of Rare Earth, Wiley, New York, 1965.
[8]. J. Mulak, Z. Gajek, The Effective Crystal Field Potential, Elsevier, Amsterdam, 2000.
[9]. R. Bo˘ca, Zero-field splitting in metal complexes, Coord. Chem. Rev. 248 (2004) 757–815.
[10]. M. G. Brik, N. M. Avram (Eds.). Optical Properties of 3d-Ions in Crystals: Spectroscopy and Crystal Field Analysis. Heidelberg: Springer, (2013), Y. Y. Yeung: Chapter 3, pp. 95-121.
[11]. [M. G. Brik, N. M. Avram, C. N. Avram, Crystal Field Analysis of Cr^{3+} Energy Levels in $LiGa_5O_8$ Spinel, Acta Phys. Polon. A112 (2007) 1055-1060.
[12]. D. J. Newman and B. Ng, The superposition model of crystal fields, Rep. Prog. Phys. 52 (1989) 699-763.
[13]. D. J. Newman, E. Siegel**,** Superposition model analysis of Fe^{3+} and Mn^{2+} spin-Hamiltonian parameters, J. Phys. C: Solid State Phys. 9 (1976) 4285-4292.
[14]. Y. Y. Yeung, Local distortion and zero-field splittings of $3d^5$ ions in oxide crystals, J. Phys. C: Solid State Phys. 21 (1988)2453-2462.
[15]. A. K. Cheetham, C. N. R. Rao, There's Room in the Middle, Science 318(2007) 58-59.
[16]. B. Li, H.-M. Wen, W. Zhou, B. Chen, Porous Metal–Organic Frameworks for Gas Storage and Separation: What, How, and Why?, J. Phys. Chem. Lett., 5(2014) 3468–3479.
[17]. J. G. Loe, I. O. Lizarán, L. F. Sanchez, J. L. Alió, N. Cuenca, A. V. Estrada, J. S. Albero, Metal–Organic Frameworks as Drug Delivery Platforms for Ocular Therapeutics, ACS Appl. Mater. Interfaces, 11(2019) 1924–1931.
[18]. Y. Tian, A. Stroppa, Y. Chai, L. Yan, S. Wang, P. Barone, S. Picozzi, Y. Sun, Cross coupling between electric and magnetic orders in a multiferroic metal-organic framework, Sci. Rep., 4(2014) 6062.
[19]. P. Jain, A. Stroppa, D. Nabok, A. Marino, A. Rubano, D. Paparo,M. Matsubara, H. Nakotte, M. Fiebig, S. Picozzi *et al.*, Switchable electric polarization and ferroelectric domains in a metal-organic-framework, npj Quantum Mater. 1(2016) 16012.
[20]. M. Maczka, A. Gagor, B. Macalik, A. Pikul, M. Ptak, J. Hanuza, Order–Disorder Transition and Weak Ferromagnetism in the Perovskite Metal Formate Frameworks of $[(CH_3)_2NH_2][M(HCOO)_3]$ and $[(CH_3)_2ND_2][M(HCOO)_3]$ (M = Ni, Mn), Inorg. Chem., 53(2014) 457–467.
[21]. D. Di Sante, A. Stroppa, P. Jain, S. Picozzi, Tuning the Ferroelectric Polarization in a Multiferroic Metal–Organic Framework, J. Am. Chem. Soc., 135(2013) 18126–18130.
[22]. P. Jain, N. S. Dalal, B. H. Toby, H. W. Kroto, A. K. Cheetham, Order−Disorder Antiferroelectric Phase Transition in a Hybrid Inorganic−Organic Framework with the Perovskite Architecture, J. Am. Chem. Soc., 130(2008) 10450–10451.
[23]. G. C. Xu, W. Zhang, X. M. Ma, Y. H. Chen, L. Zhang, H. L. Cai, Z. M. Wang, R. G. Xiong, S. Gao, Coexistence of Magnetic and Electric Orderings in the Metal–Formate Frameworks of $[NH_4][M(HCOO)_3]$, J. Am. Chem. Soc., 133(2011) 14948–14951**.**
[24]. M. Maczka, K. S. Małek, A. Ciupa, J. Hanuza, Vib. Spectrosc., **77**(2015) 17–24.
[25]. R. Shang, S. Chen, K. L. Hu, B. W. Wang, Z. M. Wang, S. Gao, A Variety of Phase-Transition Behaviors in a Niccolite Series of $[NH_3(CH_2)_4NH_3][M(HCOO)_3]_2$, Chem.: Eur. J., 22(2016) 6199–6203.
[26]. M. Maczka, A. Pietraszko, B. Macalik, K. Hermanowicz, Structure, Phonon Properties, and Order–Disorder Transition in the Metal Formate Framework of $[NH_4][Mg(HCOO)_3]$, Inorg. Chem., 53(2014) 787–794.
[27]. G. C. Xu, X. M. Ma, L. Zhang, Z. M. Wang, S. Gao**,** Disorder−Order Ferroelectric Transition in the Metal Formate Framework of $[NH_4][Zn(HCOO)_3]$, J. Am. Chem. Soc., 132(2010) 9588–9590.
[28]. Z. Wang, B. Zhang, K. Inoue, H. Fujiwara, T. Otsuka, H. Kobayashi, M. Kurmoo, Occurrence of a Rare $4^9{\cdot}6^6$ Structural Topology, Chirality, and Weak Ferromagnetism in the $[NH_4][M^{II}(HCOO)_3]$ (M = Mn, Co, Ni) Frameworks, Inorg. Chem., 46(2007) 437–445.
[29]. L. G. Aguirre, B. P. Doldán, A. Stroppa, S. Y. Vilar, L. Bayarjargal, B. Winkler, S. C. García, J. Mira, M. S. Andújar, M. S. Rodríguez, Room-Temperature Polar Order in $[NH_4][Cd(HCOO)_3]$ - A Hybrid Inorganic–Organic Compound with a Unique Perovskite Architecture, Inorg. Chem., 54(2015) 2109–2116.
[30]. M. Navickas, L. Giri¯unas, V. Kalendra, T. Biktagirov, U. Gerstmann, W. G. Schmidt, M. Maczka, A. Pöppl, J. Banys, M. Šim˙enas, Electron paramagnetic resonance study of ferroelectric phase transition and dynamic effects in a Mn^{2+} doped $[NH_4][Zn(HCOO)_3]$ hybrid formate framework, Phys. Chem. Chem. Phys. 22(2020)8513-8521._
[31]. W. L. Yu, M.G. Zhao, Spin-Hamiltonian parameters of ^6S state ions. Phys. Rev. B 37(1988) 9254-9267.
[32]. G. Aromí, E. K. Brechin, Synthesis of 3d metallic single-molecule magnets, Struct. Bonding 122 (2006) 1-67.
[33]. C. Coulon, H. Misayaka, R. Clérac, Single-Chain Magnets: Theoretical Approach and Experimental Systems, Struct. Bonding 122 (2006) 163-206.

[34]. M. Murrie, Cobalt(II) single-molecule magnets, Chem. Soc. Rev. 39 (2010) 1986-1995.
[35]. C. van Wüllen, Magnetic anisotropy through cooperativity in multinuclear transition metal complexes: theoretical investigation of an anisotropic exchange mechanism, Mol. Phys. 111 (2013) 2392–2397.
[36]. R. Batten, R. Robson, Interpenetrating Nets: Ordered, Periodic Entanglement, **Angew. Chem., Int. Ed. 37(1998) 1460-1494.**
[37]. C. J. Radnell, J. R. Pilbrow, S. Subramanian, M. T. Rogers, Electron paramagnetic resonance of Fe^{3+} ions in $(NH_4)_2SbF_5$. J. Chem. Phys. 62(1975) 4948-4952.
[38]. C. Rudowicz, R. Bramley, On standardization of the spin Hamiltonian and the ligand field Hamiltonian for orthorhombic symmetry. J. Chem. Phys. 83(1985) 5192- 5197.
[39]. B. N. Figgis, M. A. Hitchman, Ligand Field Theory and its Applications; Wiley, New York, 2000.
[40]. T. H. Yeom, S. H. Choh, M. L. Du, M. S. Jang, EPR study of Fe^{3+} impurities in crystalline $BiVO_4$. Phys. Rev. B 53(1996) 3415-3421.
[41]. T. H. Yeom, S. H. Choh, M. L. Du, A theoretical investigation of the zero-field splitting parameters for an Mn^{2+} centre in a $BiVO_4$ single crystal. J. Phys.: Condens. Matter 5(1993) 2017-2024.
[42]. C. K. Jorgensen, Modern Aspects of Ligand Field Theory; North- Holland, Amsterdam, 1971, p.305.
[43]. R. Kripal, H. Govind, S. K. Gupta, M. Arora, EPR and optical absorption study of Mn^{2+}-doped zinc ammonium phosphate hexahydrate single crystals, Physica B 392 (2007) 92-98.
[44]. D. J. Newman, B. Ng (Eds.), Crystal Field Handbook; Cambridge University Press, Cambridge, 2000.
[45]. A. Edgar, Electron paramagnetic resonance studies of divalent cobalt ions in some chloride salts. J. Phys. C: Solid State Phys. 9(1976) 4303-4314.
[46]. R. Kripal, M. G. Misra, A. K. Yadav, P. Gnutek, M. Açıkgöz, C. Rudowicz, Theoretical Analysis of Crystal field Parameters and Zero field Splitting Parameters for Mn^{2+} ions in Tetramethylammonium Tetrachlorozincate, Polyhedron, 235(2023)116341.
[47]. Y. Y. Yeung, C. Rudowicz, Crystal Field Energy Levels and State Vectors for the $3d^N$ Ions at Orthorhombic or Higher Symmetry Sites. J. Comput. Phys. 109(1993) 150-152.